

Kinetic study of inelastic radiation-induced processes in rare-gas cryocrystals

A.N. Ogurtsov, N.Yu. Masalitina, and O.N. Bliznjuk

National Technical University «KhPI», 21 Frunse Str., Kharkov 61002, Ukraine

E-mail: ogurtsov@kpi.kharkov.ua

Received October 20, 2006

The processes of large-scale atomic displacements induced by exciton self-trapping were studied using the selective vacuum ultraviolet luminescence method. Models of Frenkel pairs creation in rare-gas crystals are discussed with a focus on excited-state mechanisms of defect formation. A simple kinetic model of defect accumulation in rare-gas samples is proposed.

PACS: 61.82.Ms Insulators;
71.35.-y Excitons and related phenomena;
78.55.Hx Other solid inorganic materials.

Keywords: rare-gas crystals, self-trapping, Frenkel pairs, defect accumulation.

1. Introduction

Rare-gas cryocrystals (RGC), or atomic cryocrystals, are the model systems in physics and chemistry of solids, and a lot of information about electronic excitations in RGC has been documented in several books and Refs. 1–5. As a consequence of the closed electronic shells, solid Xe, Kr, Ar, and Ne are the simplest known solids of the smallest binding energy ε_b between atoms in the lattice. On the other hand, solid Ar and Ne have band-gap energies E_g exceeding that of LiF and may be cited as the widest band-gap insulators.

The subthreshold inelastic radiation-induced atomic processes in RGC such as defect formation and desorption under excitation by photons and electrons with a kinetic energies below the threshold of knock-on of atoms from the lattice sites were studied recently [5–10]. Our study revealed that these processes have general similarity, they are all pass through the stage of trapping or self-trapping of mobile electronic excitations and, in principle, may be considered within the context of a single kinetic model [11,12]. However, to our knowledge, the kinetic analysis of the dose curves of electronic excitation induced accumulation of crystal lattice imperfections was not done up to now. In the present paper we propose the simple kinetic model for radiation-induced defect accumulation processes, which may be used for RGC certification and comparison.

2. Experimental

The experiments were carried out at the SUPER-LUMI-station at HASYLAB, DESY, Hamburg. The selective photon excitation was performed by near-normal incidence 2 m primary monochromator with photon flux about 10^{12} photons/s at spectral resolution $\Delta\lambda = 0.2$ nm. The VUV-luminescence analysis was performed both with low-resolution, $\Delta\lambda = 2$ nm, Pouey high-flux monochromator equipped with a multisphere plate detector and with high-resolution, $\Delta\lambda = 0.1$ nm, secondary 1 m near-normal incidence monochromator equipped with a position-sensitive detector. The experimental setup and methods of sample preparation from vapor phase were described in detail elsewhere [9]. The samples had diameter 1 cm and thickness 1 mm. The irradiated area of the sample was 4×0.15 mm and to verify the reproducibility of the dose curves the several sequential independent irradiations of the same sample were performed by using of a sample movement mechanism.

3. Results and discussion

The electronic properties of RGC have been under investigation since seventies and now the overall picture of creation and trapping of electronic excitations is basically complete. Because of strong interaction with phonons the excitons and holes in RGC are self-trapped, and a wide range of electronic excitations are created in samples: free

excitons (FE), atomic-like (A-STE) and molecular-like self-trapped excitons (M-STE), molecular-like self-trapped holes (STH) and electrons trapped at lattice imperfections. The coexistence of free and trapped excitations results in the presence of a wide range of luminescence bands with well-studied internal structure in the emission spectra of RGC (Fig. 1,a). Mutual interplay and evolution in time of the intensity and shape of different luminescence bands reveal the transformation of RGC crystal properties under external effects [1–5]. On the other hand, the high sensitivity of luminescence spectra to sample growing and excitation conditions pose a real problem for comparison of data from different samples [8–10].

The most prominent feature in luminescence of Xe, Kr and Ar — the so-called *M*-band — is formed by $1,3\Sigma_u^+ \rightarrow 1\Sigma_g^+$ transitions in (R_2^*) excimer M-STE (*R* — rare gas atom). The negative electron affinity is a moving force of the cavity («bubble») formation around A-STE in the bulk of crystal, and the desorption of atoms and excimers from the surface of solid Ne and Ar [4]. Radiative «hot» transitions in desorbed excimers of Ar and Ne result in a *W*-band [2]. *A*-bands are emitted by A-STE (R^*). Recent study of charged centers in RGC reveals the nature of *H*-bands. These bands correspond to the third continua in rare gas emission, which are formed by transitions $(R_2^+)^* \rightarrow (R_2^+)$ in molecular ions. A tiny amount of impurity Xe atoms in solid Kr results in the formation of heteronuclear excited ions $(KrXe^+)^*$ and a corresponding *H'*-band [5]. Radiative decay of free excitons from the bottom of the lowest $\Gamma(3/2)$, $n = 1$ excitonic band produces strong lines (FE) in spectra of solid Xe, Kr and Ar [2, 13].

The analysis of the luminescence spectra of rare-gas cryocrystals under different excitation conditions, excitation energies and crystal-growth conditions made it possible to elucidate the internal structure of *M*- and *A*-bands.

Each of the *M*-bands can be well approximated by two components (Fig. 1,b): low energy subband M_1 and high energy one M_2 [7]. The subband M_2 is dominant in the luminescence of more perfect samples. The spectra of samples with a great number of initial defects are mainly determined by the component M_1 . This suggests that the subband M_2 is emitted by the excitons, which are self-trapped in the regular lattice, while the component M_1 is emitted by the centers, which are populated during trapping, that occurs with the lattice imperfections involved. The excitation spectra of the M_1 - and M_2 -subbands were restored by decomposing the sequence of the luminescence spectra measured at different excitation energies [7]. Using the restored excitation spectra the threshold energies for the M_1 and M_2 subbands to appear were determined. In all cases the excitation spectra of the M_1 -subbands exhibit preferential excitation at energies below the $n = 1$ exciton and prove a direct photoabsorption by defect-related centers that produces the only M_1 component in the spectra [14]. In all cases the transformation of the *M*-band due to sample annealing or irradiation, resulting in the lattice degradation, may be described by the intensity redistribution between two subbands M_1 and M_2 .

The *A*-bands of solid Ar and Ne have two main subbands A_1 and A_2 (Fig. 1,b). The band of the bulk emission associated with the transition $3P_1 \rightarrow 1S_0$ consists of a high-energy component A_2 stemmed from A-STE in a regular lattice and a low-energy one, A_1 , which appears to be associated with structural defects. Additional subband A_0 stems from desorbed atoms. The *d* component assigns to emission from metastable $3P_2$ state. In previous papers [5, 15] the subbands *d*, A_0 , A_1 , A_2 were marked as *d*, b_0 , b_1 , b_2 . Similar structure has *A*-band of solid Ar [13].

The interatomic bond scission in the crystal lattice may be stimulated either by elastic encounters between

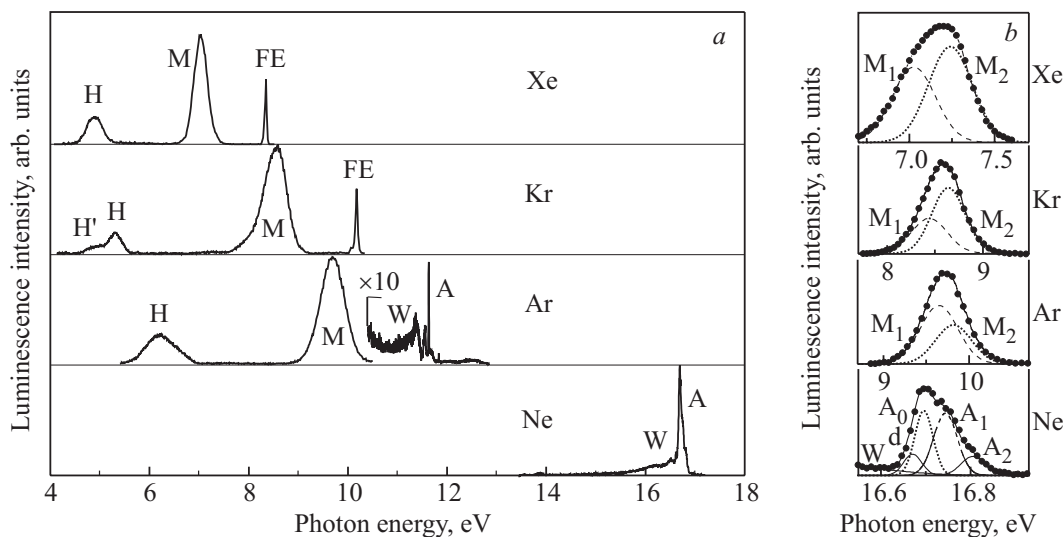


Fig. 1. Photoluminescence spectra of rare-gas cryocrystals at $T = 5$ K. General view under excitation by photons with energies $h\nu = E_g$ (a). Internal structure of luminescence bands under excitation by photons with energies: $h\nu_{Xe} = 9.15$ eV, $h\nu_{Kr} = 11.21$ eV, $h\nu_{Ar} = 13.57$ eV, $h\nu_{Ne} = 20$ eV (b).

atoms composing solids and incoming particles or by creation of electronic excitations which transfer the energy to a specified crystal cell. The energy stored by electronic excitations in RGC is much higher than the binding energy ε_b and various trapping processes concentrate the energy within a volume of about a unit cell. The extremely high quantum yield of luminescence [16] allows one to neglect non-radiative transitions, and the population of antibonding $^1\Sigma_g^+$ ground molecular state is usually considered as a main source of kinetic energy for a large-scale movement of atoms finishing in the Frenkel defects or desorption of atoms in the ground state — the ground-state (GS) mechanism. On the other hand, the processes of formation of A-STE and M-STE centers themselves are accompanied by a considerable energy release to the crystal lattice, which also exceeds the binding energy ε_b [5]. Since the energy of STE is transferred into kinetic energy of atomic motion over a unit cell, the formation of three-, two-, or one-dimensional defects is ruled out. In our case, only the point defects, Frenkel-pairs, may emerge in the bulk of the crystal. Such an excited-state (ES) mechanism of the large-scale atomic movement was studied recently [5,15,17]. Fig. 2 illustrates this process schematically. The excited-state mechanism of M-STE to Frenkel pair conversion in solid Xe, Kr and Ar is supposed to occur by self-trapping of exciton in perfect lattice (Fig. 2,a,b), and displacement of M-STE from centrosymmetric position in the $\langle 110 \rangle$ direction and re-orientation to the $\langle 100 \rangle$ direction to stabilize the defect (Fig. 2,b,c) [17,18]. In the case of solid Ne the excited-state mechanism of A-STE to Frenkel pair conversion occurs by self-trapping of exciton in the perfect lattice (Fig. 2,d,e), accompanied by the strong repulsion of the Rydberg electron of excited atom with a closed shell of surrounding atoms and substantial local lattice rearrange-

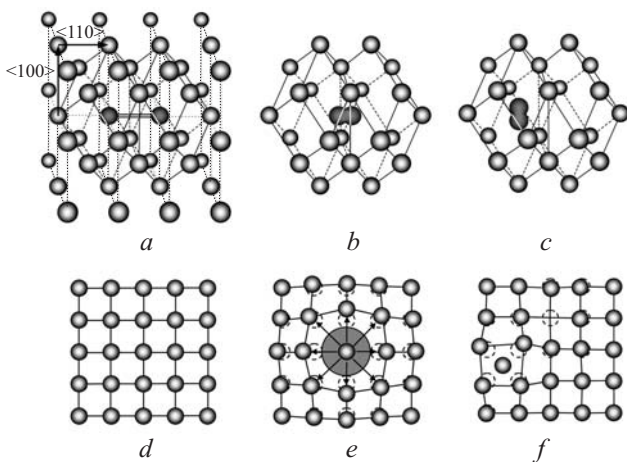


Fig. 2. Scheme of the «excited state» mechanism of Frenkel-pair formation induced by exciton self-trapping: into molecular state (a), (b), (c) and into atomic state (d), (e), (f).

ment, which leads to a «bubble» formation around the excited atom [15]. After the bubble formation the surrounding ground state atoms are moved to the second shell and second-nearest neighboring vacancy-interstitial pairs could create the permanent defects [19], which remain in the lattice after exciton annihilation (Fig. 2,e,f). The time (or dose) dependences of the «defect» components «1» — the progress curves of the process of defect formation — turned out to be a very precise and sensitive tool to study the defect accumulation processes in rare-gas cryocrystals [5]. Figs. 3 and 4 show examples of such progress curves of solid Xe and Ne under irradiation by photons with energies $E < E_g$ [5,15]. An increase in the intensity of the defect component during irradiation reflects the accumulation of stable long-lived defects in the lattice as a result of exciton creation and self-trapping. Dose curves are saturated at long time of irradiation. Additional source of Frenkel pairs under irradiation by photons with energies $E > E_g$ is a hole self-trapping [4], which is also accompanied by creation of a metastable trapped centers [20] and shows a pronounced dose dependence of H-band [21].

In all cases we can consider the process of defect formation as a combination of three separate processes:



Process (1) is a trapping of mobile excitation, E , with a rate constant k_1 , on trapping center, T , and formation of an excited metastable trapped center MTE (A-STE, M-STE, or STH), which may be considered as metastable short-lived lattice defect. Schematically the process (1)

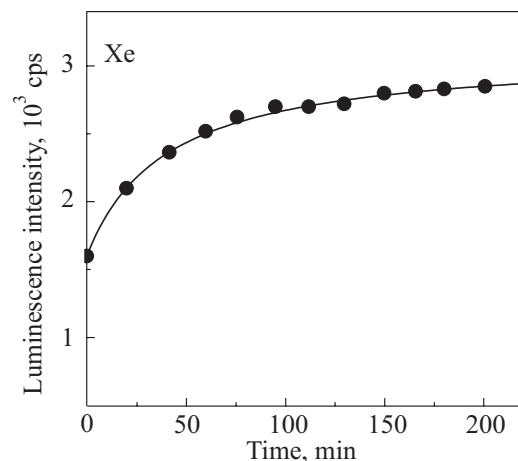


Fig. 3. Dose dependence of subband M_1 of solid Xe excited by photons with $h\nu = 9.15$ eV (dots) and fitting by Eq. (4) (solid curve).

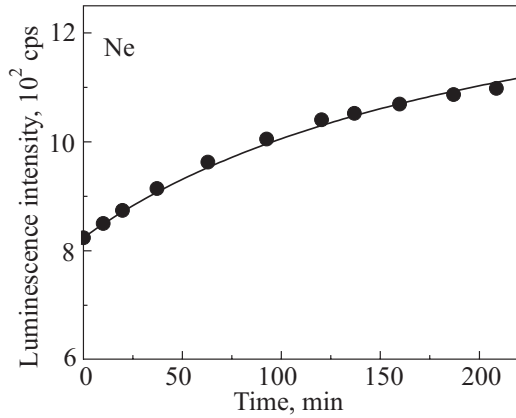


Fig. 4. Dose dependence of subband A_1 of solid Ne excited by photons with $h\nu=20$ eV (dots) and fitting by Eq. (4) (solid curve).

corresponds to change Fig. 2, *a,b* in the case of exciton self-trapping into molecular state, or Fig. 2, *d,e* in the case of exciton self-trapping into atomic state. Radiative decay of the short-lived MTE-center either returns the lattice with a rate constant k_{-1} into the initial state without permanent defect (process (2), transformations $b \rightarrow a$ and $e \rightarrow d$ in Fig. 2 for molecular and atomic self-trapped excitons, correspondingly), or forms the permanent defect D (Frenkel pair) in the process (3) with a rate constant k_2 (transformations $b \rightarrow c$ and $e \rightarrow f$ in Fig. 2 for molecular and atomic self-trapped excitons, correspondingly). We assume that low level of irradiation under steady state conditions creates a constant low concentration of mobile excitations, N_0 , which is less than concentration of the trapping centers, $n_T > N_0$, and at the beginning of irradiation (concentration of defects n_D is small), defect concentration grows linearly with time, $n_D = At$ ($A = \text{const}$). Linear growth of «1»-subbands at the beginning of irradiation was experimentally detected in all experiments. The rate equation for a number of MTE-centers per irradiated volume, n_{MTE} , is $dn_{MTE}/dt = k_1 n_E n_T - k_{-1} n_{MTE} - k_2 n_{MTE}$ [11]. Irradiation-produced electronic excitations may be either free, or trapped, $N_0 = n_E + n_{MTE}$. On the basis of these assumptions the time dependence of luminescence intensity of «defect» subband $I_1(t)$ under steady-state conditions may be expressed in a form

$$I_1(t) = I_1(0) + \frac{Kt}{L+t}, \quad (4)$$

where $I_1(0)$ is the initial intensity of «defect» luminescence due to $n_D \neq 0$ at $t=0$ [10], $K = k_2 N_0$ is the saturation value of $I_1(t) - I_1(0)$ at $t \rightarrow \infty$, $L = (k_{-1} + k_2) / (k_1 A)$ is a characteristic constant of a sample — under identical excitation and detection conditions the sample with less pronounced processes of defect formation will have a higher value of L .

Figures 3 and 4 show the examples of fitting by Eq. (4) the dose curves of «defect» components «1» of solid Xe and Ne. The fitting values of constants are $K_{Xe} = 1500$ cps, $K_{Ne} = 620$ cps, $L_{Xe} = 40$ min, $L_{Ne} = 230$ min, which is in line with general increase of defect formation efficiency in the sequence Ne, Ar, Kr, Xe [4]. Linear transformation of Eq. (4) in the form $(I_1(t) - I_1(0))^{-1} = K^{-1} + L(Kt)^{-1}$ allows one to determine the values of constants K and L from interceptions with axis of double reciprocal plot of the straight line of data linear fit. Analytical application of the model enables one to compare different rare-gas crystals with standard crystals and estimate the radiation doses from initial part of the dose curves [12].

In summary, the selective excitation of excitons in rare-gas cryocrystals by photons with energies $E < E_g$ results in accumulation of Frenkel pairs by intrinsic excited-state mechanism of defect formation via self-trapping of excitons. The proposed kinetic model allows fitting the experimental dose dependences of «defect» subbands and obtaining the particular kinetic parameters. This approach provides a way of qualitative and quantitative analysis and certification of rare-gas crystals, which is indispensable at any attempt of comparison of data from different samples.

1. N. Schwentner, E.-E. Koch, and J. Jortner, *Electronic Excitations in Condensed Rare Gases*, Springer-Verlag, Berlin (1985).
2. G. Zimmerer, in: *Excited-State Spectroscopy in Solids*, U.M. Grassano and N. Terzi (eds.), North-Holland, Amsterdam (1987).
3. I.Ya. Fugol, *Adv. Phys.* **37**, 1 (1988).
4. K.S. Song and R.T. Williams, *Self-Trapped Excitons*, Springer-Verlag, Berlin (1996).
5. A.N. Ogurtsov, in: *Spectroscopy of Emerging Materials*, E. Faulques et al. (eds.), Kluwer, Dordrecht (2004).
6. A.N. Ogurtsov, E.V. Savchenko, J. Becker, M. Runne, and G. Zimmerer, *J. Luminesc.* **76–77**, 478 (1998).
7. A.N. Ogurtsov and E.V. Savchenko, *J. Low Temp. Phys.* **122**, 233 (2001).
8. A.N. Ogurtsov, E.V. Savchenko, S. Vielhauer, and G. Zimmerer, *J. Luminesc.* **112**, 97 (2005).
9. A.N. Ogurtsov, E.V. Savchenko, E. Sombrowski, S. Vielhauer, and G. Zimmerer, *Fiz. Nizk. Temp.* **29**, 1125 (2003) [*Low Temp. Phys.* **29**, 858 (2003)].
10. A.N. Ogurtsov, in: *Integrated Technologies and Energy Saving*, NTU, Kharkov (2005).
11. H. Schmalzried, *Chemical Kinetics of Solids*, VCH Verlag, Weinheim (1995).
12. R.W. Balluffi, S.M. Allen, and W.C. Carter, *Kinetics of Materials*, Wiley-Interscience, Hoboken (2005).
13. I.Ya. Fugol, E.V. Savchenko, Yu.I. Rybalko, and A.N. Ogurtsov, *Fiz. Nizk. Temp.* **12**, 773 (1986) [*Sov. J. Low Temp. Phys.* **12**, 439 (1986)].

14. A.N. Ogurtsov, G. Stryganyuk, S. Vielhauer, and G. Zimmerer, in: *HASYLAB Annual Report 2004*, Hamburg, DESY (2005).
15. E.V. Savchenko, A.N. Ogurtsov, and G. Zimmerer, *Fiz. Nizk. Temp.* **29**, 356 (2003) [*Low Temp. Phys.* **29**, 270 (2003)].
16. D.E. Grosjean, R.A. Vidal, R.A. Baragiola, and W.L. Brown, *Phys. Rev.* **B56**, 6975 (1997).
17. E. Savchenko, A. Ogurtsov, I. Khyzhniy, G. Stryganyuk, and G. Zimmerer, *Phys. Chem. Chem. Phys.* **7**, 785 (2005).
18. E.V. Savchenko, A.N. Ogurtsov, O.N. Grigorashchenko, and S.A. Gubin, *Chem. Phys.* **189**, 415 (1994).
19. C. Fu and K.S. Song, *J. Phys. Condens. Matter* **9**, 9785 (1997).
20. A.N. Ogurtsov, E.V. Savchenko, M. Kirm, B. Steeg, and G. Zimmerer, *J. Electron Spectrosc. Relat. Phenom.* **101–103**, 479 (1999).
21. O.N. Grigorashchenko, S.A. Gubin, A.N. Ogurtsov, and E.V. Savchenko, *J. Electron Spectrosc. Relat. Phenom.* **79**, 107 (1996).